

# Estimating Brain Conductivities and Dipole Source Signals With EEG Arrays

David Gutiérrez, Arye Nehorai\*, *Fellow, IEEE*, and Carlos H. Muravchik, *Senior Member, IEEE*

**Abstract**—Techniques based on electroencephalography (EEG) measure the electric potentials on the scalp and process them to infer the location, distribution, and intensity of underlying neural activity. Accuracy in estimating these parameters is highly sensitive to uncertainty in the conductivities of the head tissues. Furthermore, dissimilarities among individuals are ignored when standardized values are used. In this paper, we apply the maximum-likelihood and *maximum a posteriori* (MAP) techniques to simultaneously estimate the layer conductivity ratios and source signal using EEG data. We use the classical 4-sphere model to approximate the head geometry, and assume a known dipole source position. The accuracy of our estimates is evaluated by comparing their standard deviations with the Cramér-Rao bound (CRB). The applicability of these techniques is illustrated with numerical examples on simulated EEG data. Our results show that the estimates have low bias and attain the CRB for sufficiently large number of experiments. We also present numerical examples evaluating the sensitivity to imprecise assumptions on the source position and skull thickness. Finally, we propose extensions to the case of unknown source position and present examples for real data.

**Index Terms**—Brain conductivities, Cramér-Rao bound, electroencephalography, maximum-likelihood estimation, parameter estimation, sensor array processing.

## I. INTRODUCTION

THE PROBLEM of dipole source localization and signal estimation is of great interest in neuroscience. It has applications in areas such as clinical sciences and brain research [1]. Techniques based on electroencephalography (EEG) measure the electric potentials on the scalp and process them to infer the location and signal of the underlying neural activity. Solution to this inverse problem requires knowledge of the conductivities of the different layers in the head. It has been shown that accuracy of estimating the source parameters is highly sensitive to the uncertainty in the conductivities of most of the head tissues [2]. These conductivities are typically obtained by direct measurements of *in vivo* and *in vitro* samples of the tissues involved [3]. Then, dissimilarities in the conductivities among individuals

are ignored. Other methods such as impedance tomography [4], [5], and magnetic resonance using current density imaging [6] allow individual estimation, but they require each patient to be a subject of a study for estimating his/her tissues' conductivities before, and in addition to, the EEG measurements. Recently, magnetic resonance diffusion-weighted imaging techniques have been developed to estimate conductivities on an individual basis [7]. Simultaneous magnetoencephalography (MEG) and EEG analysis has been used to derive "equivalent" conductivity estimates that improve the estimation of dipole source parameters [8].

In this paper (see, also, [9]), we develop statistical methods that allow simultaneous estimation of the ratios of the layer conductivities and source signal using EEG array data. In Section II, we give a general description of the dipole source model. There, we assume the classical concentric 4-sphere model to approximate the head geometry. This model is justified for sources near the surface [10]. More realistic head models would require a numerical solution, which is computationally more intensive, using boundary element (BEM) [11] or finite element (FEM) [12] methods based on individual head geometries. In our case, we assume also that the geometry of the head's layers and the position of the source are known. The assumption of known dipole position holds for certain evoked response and event-related experiments [13]. In these cases, the response is approximately a predictable and repetitive equivalent current dipole with known location.

In Section III, we propose two estimation methods. The first one is based on the maximum-likelihood (ML) technique, which is asymptotically efficient under general regularity conditions [16]. In the second method, we obtain the maximum *a posteriori* (MAP) estimate under the consideration of random conductivity parameters with known *a priori* distribution. Section III also defines the Cramér-Rao bounds (CRBs) for both ML and MAP estimates. The CRB is useful as it provides a universal reference for evaluating the performance of unbiased estimates [17], [18]. In Section IV, experiments with simulated and real data are used to demonstrate the applicability of our methods to a practical EEG measurement system. Furthermore, we propose two alternative procedures for cases when the assumption of known position does not hold. In the first procedure, we obtain an estimate of the position using MEG techniques (see also [14] and [15]). For the second, we use EEG only to estimate the position and the conductivities iteratively. Section IV also presents numerical examples evaluating the sensitivity of the estimates to wrong specification of the source position or variations in the skull's thickness. This sensitivity analysis is useful to study the robustness of the proposed estimation algorithms. In Section V, we discuss the results, limitations, and further work.

Manuscript received November 26, 2002; revised April 18, 2004. This work was supported in part by the Air Force Office of Scientific Research under Grant F49620-02-1-0339, and in part by the National Science Foundation under Grant CCR-0105334 and Grant CCR-0330342. The work of C. H. Muravchik was supported in part by the ANPCyT, CIC-PBA, and UNLP. *Asterisk indicates corresponding author.*

D. Gutiérrez is with the Department of Bioengineering, University of Illinois at Chicago, Chicago, IL 60607-7053 USA (e-mail: dgutie7@uic.edu).

\*A. Nehorai is with the Department of Electrical and Computer Engineering, University of Illinois at Chicago, Chicago, IL 60607-7053 USA (e-mail:nehorai@ece.uic.edu).

C. H. Muravchik is with the Laboratorio de Electrónica Industrial Control e Instrumentación, Departamento Electrotecnia, Facultad de Ingeniería, University Nacional de La Plata, La Plata, Argentina (e-mail: carlosm@ing.unlp.edu.ar).

Digital Object Identifier 10.1109/TBME.2004.836507

## II. FORWARD MODEL

In this section, we discuss the forward problem of computing the surface potential for a dipole source. The geometry of the head and the location of the source are assumed to be known.

For the head model, we choose a multishell spherical model which includes four concentric layers for the brain, cerebrospinal fluid (CSF), skull, and scalp. These layers are considered to be isotropic and to have homogeneous conductivities  $\sigma_1, \dots, \sigma_4$ , and radii  $\rho_1, \dots, \rho_4$ , respectively. This type of model is often used to simplify the calculations in modeling electrical activity in the brain [19].

Consider a single dipole with a moment  $\tilde{\mathbf{q}} = [\tilde{q}_x, \tilde{q}_y, \tilde{q}_z]^T$  located at a point  $\mathbf{p} = [p_x, p_y, p_z]^T$  in the brain. The surface potential at the  $i$ th sensor located on the scalp at  $\mathbf{r}_i = [r_{ix}, r_{iy}, r_{iz}]^T$ ,  $i = 1, \dots, m$ , where  $m$  is the number of electrodes, can be expressed as

$$v_i = \mathbf{g}_i^T(\boldsymbol{\theta})\mathbf{q} \quad (1)$$

where  $\mathbf{q} = \tilde{\mathbf{q}}/\sigma_4$ ,  $\mathbf{g}_i(\boldsymbol{\theta})$  is the gain vector (or ‘‘field kernel’’), and  $\boldsymbol{\theta} = [\theta_1, \theta_2, \theta_3]^T$  the parameter vector defined by the ratios of the conductivities,  $\theta_j = \sigma_j/\sigma_{j+1}$ ,  $j = 1, \dots, 3$ , which corresponds to the ratios going from the inner to the outer layer of our head model.

Under the above conditions, we can express  $\mathbf{g}_i$  for our 4-layer model as [20]

$$\mathbf{g}_i(\boldsymbol{\theta}) = \frac{1}{4\pi\rho_4^2} \sum_{n=1}^{\infty} w(\boldsymbol{\theta}; \rho_1, \dots, \rho_4; n) \left( \frac{\|\mathbf{p}\|}{\rho_4} \right)^{n-1} \times \left[ \mathbf{r}_o P_n(\cos \varphi_i) + \mathbf{t}_o \frac{P_n^1(\cos \varphi_i)}{n} \right] \quad (2)$$

where  $P_n(\cdot)$  is the Legendre polynomial of order  $n$ ;  $P_n^1(\cdot)$  is the associated Legendre Polynomial;  $\mathbf{r}_o = \mathbf{p}/\|\mathbf{p}\|$ , and  $\mathbf{t}_o = (\mathbf{p} \times \mathbf{r}_i \times \mathbf{p})/\|\mathbf{p} \times \mathbf{r}_i \times \mathbf{p}\|$  are the radial and tangential unitary vectors, respectively;  $\varphi_i$  denotes the angle between  $\mathbf{r}_i$  and  $\mathbf{p}$ ; the weighting function  $w(\boldsymbol{\theta}; \rho_1, \dots, \rho_4; n)$  is defined in [10].

Define the array response as a matrix  $A(\boldsymbol{\theta})$  of size  $m \times 3$  where the  $i$ th row corresponds to  $\mathbf{g}_i^T$ . Then, we can express the potential vector  $\mathbf{v} = [v_1, \dots, v_m]^T$  measured by the  $m$  electrodes as  $\mathbf{v} = A(\boldsymbol{\theta})\mathbf{q}$ . This model can be extended to a *spatio-temporal* representation by allowing  $\mathbf{q}$  to change in time. Then, assuming the source remains at the same position during the measurements period, we have

$$\mathbf{v}(t) = A(\boldsymbol{\theta})\mathbf{q}(t). \quad (3)$$

## III. THE PROPOSED METHODS

In this section, we derive the estimation methods for finding the conductivity ratios  $\boldsymbol{\theta}$  and dipole signal  $\mathbf{q}(t)$  using EEG measurements. We first describe the corresponding methods for one source and later extend them to multiple sources.

Let  $\mathbf{y}(t)$  denote the  $m \times 1$  measurement vector obtained from the EEG sensors at time  $t$ . Assume that the measurements are

in discrete time, and are taken in the presence of zero mean Gaussian noise  $\mathbf{e}(t)$  uncorrelated in time and space and with variance  $\sigma^2$  independent of time. Then, the measurement model is given by

$$\mathbf{y}(t) = A(\boldsymbol{\theta})\mathbf{q}(t) + \mathbf{e}(t), \quad t = 1, \dots, N. \quad (4)$$

where  $N$  is the number of time samples. Observe that it is possible to estimate only the conductivity ratios  $\boldsymbol{\theta}$  and signal  $\mathbf{q}(t)$ . Simultaneous estimation of  $[\sigma_1, \sigma_2, \sigma_3, \sigma_4]^T$  and  $\tilde{\mathbf{q}}(t)$  is not possible since it would result in a nonidentifiable problem [21]. Thus, we will refer to  $\boldsymbol{\theta}$  and  $\mathbf{q}(t)$  as the conductivities and dipole signal, respectively.

### A. Deterministic Maximum-Likelihood (ML) Estimate

The problem of estimating  $\boldsymbol{\theta}$  and  $\mathbf{q}(t)$  from (4) can be seen as that of estimating these deterministic parameters from a Gaussian model. The ML estimate (MLE) of  $\boldsymbol{\theta}$  is given by

$$\hat{\boldsymbol{\theta}}_{\text{ML}} = \arg \left\{ \min_{\boldsymbol{\theta}} f(\boldsymbol{\theta}) \right\} \quad (5)$$

where  $f(\boldsymbol{\theta})$  is the concentrated likelihood function (CLF), defined as

$$f(\boldsymbol{\theta}) = \text{tr} \left\{ (I - A(A^T A)^{-1} A^T) \hat{R} \right\} \quad (6)$$

where  $A$  is used instead of  $A(\boldsymbol{\theta})$  for notational convenience,  $\text{tr}\{\cdot\}$  is the trace operator, and  $\hat{R}$  is a consistent estimate of the covariance matrix of the observation vector, defined as

$$\hat{R} = \frac{1}{N} \sum_{t=1}^N \mathbf{y}(t)\mathbf{y}(t)^T. \quad (7)$$

The CLF is a commonly used simplification for the ML technique, as it has the main advantage of reducing the dimension of the optimization problem. In our case, the log-likelihood function of the measurements was concentrated with respect to  $\sigma$  and  $\mathbf{q}(t)$  by substituting them with their corresponding ML estimates. More details on the derivation of the CLF can be found in [22].

The MLE of the dipole signal can then be obtained by a simple least-squares fit, i.e.,

$$\hat{\mathbf{q}}(t) = \left( \hat{A}^T \hat{A} \right)^{-1} \hat{A}^T \mathbf{y}(t), \quad (8)$$

where  $\hat{A}$  denotes the MLE of  $A$  (i.e.,  $\hat{A} = A(\hat{\boldsymbol{\theta}})$ ).

### B. Deterministic Cramér-Rao Bound

The CRB provides a benchmark against which we can compare the performance of any unbiased estimator. It has been shown in [22] that, for our case, the CRB is given by

$$\text{CRB}_{\text{D}}(\boldsymbol{\theta}) = \sigma^2 \Delta^{-1} \quad (9)$$

where

$$\Delta = \sum_{t=1}^N Q^T(t) D^T [I - A(A^T A)^{-1} A^T] D Q(t) \quad (10)$$

$Q(t) = I_3 \otimes \mathbf{q}(t)$ , “ $\otimes$ ” denotes the Kronecker product, and

$$D = \left[ \frac{\partial A(\boldsymbol{\theta})}{\partial \theta_1}, \frac{\partial A(\boldsymbol{\theta})}{\partial \theta_2}, \frac{\partial A(\boldsymbol{\theta})}{\partial \theta_3} \right]. \quad (11)$$

In a realistic scenario, as the one discussed in Section IV-C,  $\sigma^2$  is not available. For this case, an estimate can be computed as

$$\hat{\sigma}^2 = \frac{1}{m} \text{tr} \left\{ \left( I - \hat{A}(\hat{A}^T \hat{A})^{-1} \hat{A}^T \right) \hat{R} \right\}. \quad (12)$$

### C. Bayesian Approach

Consider the case when an approximate description of the unknown parameters is available. This description, obtained from previous experience, defines an *a priori* probabilistic distribution. With this information, we can express  $\boldsymbol{\theta}$  as a random parameter with a known *a priori* distribution  $h(\boldsymbol{\theta})$ , and use the Bayesian approach to estimate it [17]. Such an estimate is called the maximum a-posteriori (MAP) estimate, which is obtained by minimizing the following negative log-likelihood function:

$$J(\boldsymbol{\theta}) = -[\ln u(\mathbf{y}|\boldsymbol{\theta}) + \ln h(\boldsymbol{\theta})] \quad (13)$$

where the first term corresponds to the value of the distribution of  $\mathbf{y}$  for a fixed value of  $\boldsymbol{\theta}$ , and the second describes the *a priori* knowledge on the distribution of  $\boldsymbol{\theta}$ .

In our case, (13) can be seen as an extension of (6), where the CLF of the MLE is augmented with a term corresponding to the negative log-likelihood of the prior distribution. Then, we can write the Bayesian likelihood as

$$J(\boldsymbol{\theta}) = mN \ln f(\boldsymbol{\theta}) - \ln h(\boldsymbol{\theta}) \quad (14)$$

and our MAP estimate ( $\hat{\boldsymbol{\theta}}_{\text{MAP}}$ ) is given by

$$\hat{\boldsymbol{\theta}}_{\text{MAP}} = \arg \left\{ \min_{\boldsymbol{\theta}} J(\boldsymbol{\theta}) \right\}. \quad (15)$$

For the case of a multivariate Gaussian prior model distributed as  $\boldsymbol{\theta} \sim \mathcal{N}(\bar{\boldsymbol{\theta}}, \Upsilon)$ , we can easily show that (14) can be written as

$$J(\boldsymbol{\theta}) = mN \ln f(\boldsymbol{\theta}) + \frac{1}{2}(\boldsymbol{\theta} - \bar{\boldsymbol{\theta}})^T \Upsilon^{-1}(\boldsymbol{\theta} - \bar{\boldsymbol{\theta}}). \quad (16)$$

Note that the idea of introducing *a priori* information into the estimation process can be also applied to other parameters, such as  $\mathbf{p}$  or  $\rho_j$ .

### D. Stochastic Cramér-Rao Bound

For the case of random  $\boldsymbol{\theta}$ , the CRB must incorporate the stochastic content of the prior distribution. If we consider that  $\boldsymbol{\theta}$  is distributed as  $\boldsymbol{\theta} \sim \mathcal{N}(\bar{\boldsymbol{\theta}}, \Upsilon)$ , our stochastic CRB is given by

$$\text{CRB}_{\text{S}}(\boldsymbol{\theta}) = \sigma^2 \{ \sigma^2 \Upsilon^{-1} + \Delta \}^{-1}, \quad (17)$$

with  $\Delta$  as previously defined in (10). A derivation of (17) is presented in [23].

### E. Multiple Sources

For  $k$  distinct dipoles, (4) holds with  $\mathbf{q}$  and  $A(\boldsymbol{\theta})$  substituted with  $\mathbf{q} = [\mathbf{q}_1, \mathbf{q}_2, \dots, \mathbf{q}_k]^T$ , and  $A(\boldsymbol{\theta}) = [A_1(\boldsymbol{\theta}), A_2(\boldsymbol{\theta}), \dots, A_k(\boldsymbol{\theta})]$ , where

$$A_l(\boldsymbol{\theta}) = \begin{bmatrix} \mathbf{g}_{1l}^T(\boldsymbol{\theta}) \\ \mathbf{g}_{2l}^T(\boldsymbol{\theta}) \\ \vdots \\ \mathbf{g}_{ml}^T(\boldsymbol{\theta}) \end{bmatrix} \quad (18)$$

and  $\mathbf{g}_{il}$  denotes the gain vector corresponding to the  $i$ th sensor and  $l$ th dipole, for  $l = 1, \dots, k$ . Under these conditions, the MLE for  $\boldsymbol{\theta}$  and  $\mathbf{q}$  can be calculated using (5) and (8), respectively. The above substitutions also allow us to use (9) for computing the deterministic CRB. For the MAP estimate, it can be calculated by using these substitutions in (15), and the stochastic CRB is computed by (17).

## IV. NUMERICAL EXAMPLES

We conducted a series of simulations for EEG measurements in the above 4-layer spherical head model in order to illustrate the performance of our methods for practical systems. Later, in Section IV-C, we apply the ML method to real MEG/EEG data from two normal subjects.

For the simulated EEG measurements, the nominal radii of the 4 layers corresponding to the brain, CSF, skull, and scalp, were chosen to be  $[\rho_1, \rho_2, \rho_3, \rho_4] = [7.1, 7.2, 7.9, 8.5]$  cm. To simulate our source, we chose a current dipole located at  $\mathbf{p} = [5.936, 1.5352, 3.4798]^T$  cm. The components  $\tilde{q}_x$ ,  $\tilde{q}_y$ , and  $\tilde{q}_z$  of the dipole change in time according to

$$\tilde{q}_x(t) = 30e^{-((t/50)-4)^2} - 130e^{-((t/50)-6)^2} \text{ [mA} \cdot \text{cm]} \quad (19a)$$

$$\tilde{q}_y(t) = 0 \quad (19b)$$

$$\tilde{q}_z(t) = 150e^{-((t/50)-6)^2} - 50e^{-((t/50)-4)^2} \text{ [mA} \cdot \text{cm]}. \quad (19c)$$

In this set of equations,  $t$  is continuous and with units of milliseconds. We sampled these signals at a frequency of 200 Hz thus obtaining  $N = 100$  samples for our computer simulations.

For the conductivities, we used  $[\sigma_1, \sigma_2, \sigma_3, \sigma_4] = [0.33, 1, 0.0042, 0.33]$  S/m, which sets the real value of our parameter as  $\boldsymbol{\theta}_0 = [0.33, 238.095, 0.012727]^T$ . For the measurements, we used a standard 10–10 EEG configuration of  $m = 81$  electrodes. All these values were selected from previous studies in the area (see e.g., [23], [24]). The 10–10 arrangement allows consistent testing for EEG recordings as it complies with the international electrode placement system and is widely used in clinical applications [25].

### A. Signal-to-Noise Ratio (SNR) Analysis

In order to evaluate the performance of our estimates under different SNR values, we added uncorrelated (in time and space) random noise, distributed as  $\mathcal{N}(0, \sigma^2)$ , where  $\sigma$  took values from 7.08  $\mu\text{V}$  to 70.8  $\mu\text{V}$  (which corresponds to 0.1 to 1 times the mean value of the 81 measurement channels' RMS

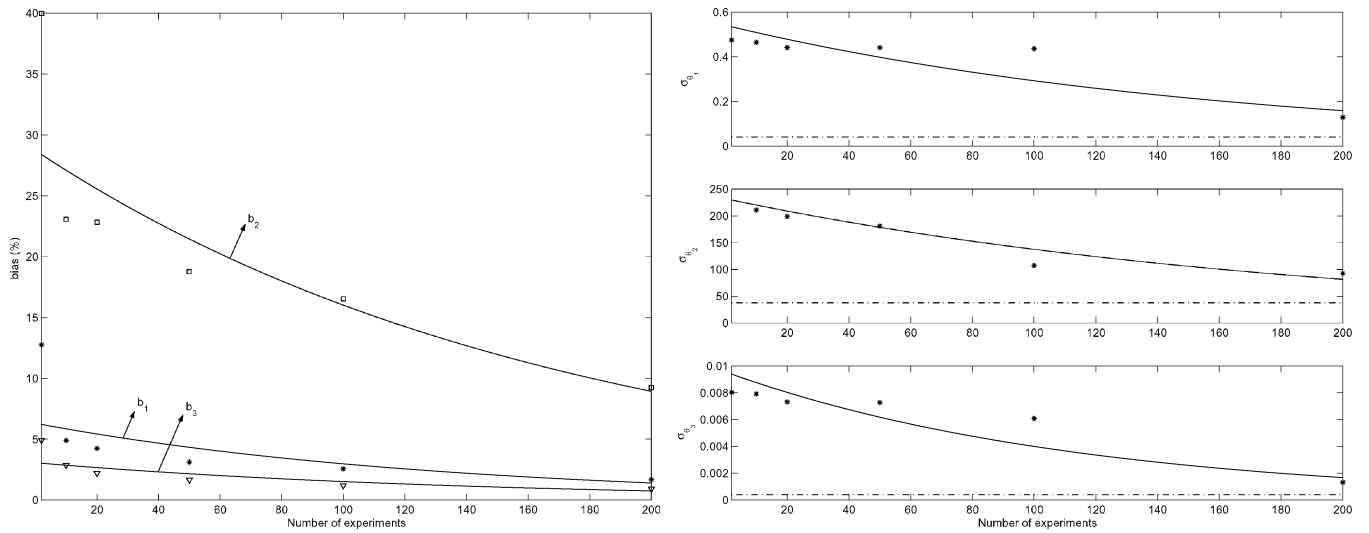


Fig. 2. Left: Bias of the ML conductivity estimates as a function of the number of experiments. Right: Standard deviations of these estimates (full lines) compared with the Cramér-Rao bound square roots (dashdotted lines).

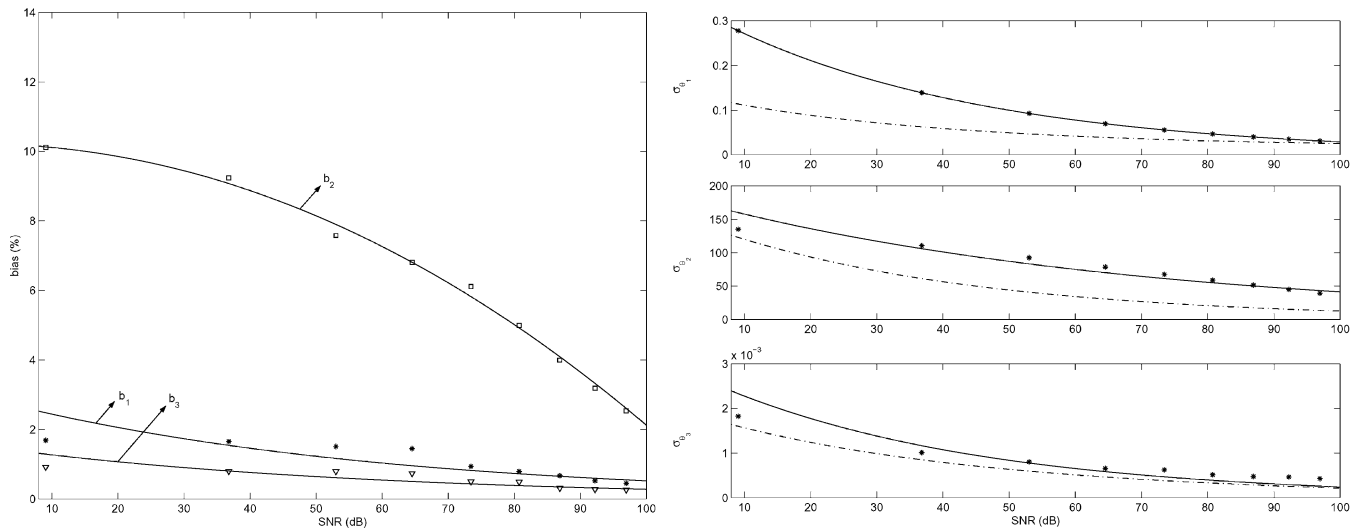


Fig. 1. Left: Bias of the ML conductivity estimates as a function of SNR. Right: Standard deviations of these estimates (full lines) compared with the Cramér-Rao bound square roots (dashdotted lines).

voltages). Then, we defined the SNR in decibels as  $SNR = 20 \log((1/m) \sum_{i=1}^m s_i^2 / \sigma^2)$ , with  $s_i^2 = (1/N) \sum_{t=1}^N v_i^2(t)$  and  $v_i(t)$  as defined in (3). Under these conditions, we calculated the ML and MAP estimates.

1) *ML Estimates:* Using the model (4), we generated our numerical data. Then, through computer implementations of (5)–(8), we calculated the deterministic ML estimates for the conductivities and dipole signal. For the implementation of (2) we used the efficient algorithm described in [24] as it provides with a very accurate closed-form approximation of the infinite sum involved.

We initialized the minimization process in (5) with the true value  $\theta_0$  in order to study the error produced by modeling factors and also to avoid the problem of local minimization. The

global minimization problem is beyond the scope of this article, however, a global estimate can be obtained, for example, with optimization methods based on genetic algorithms or multiple starting points.

For the estimation process, we repeated the experiment 200 times with independent noise realizations. Then, we computed the bias (relative error) of our estimates as  $b = |\hat{\theta}_m - \theta_0|$ , where  $\hat{\theta}_m$  is the mean estimate of the 200 experiments. The corresponding bias curves (in percent) are shown in Fig. 1. For the same set of experiments, we compared the standard deviations of the estimates (denoted as  $\sigma_{\theta_j}$ ) with the deterministic CRB square roots. The resulting curves are also shown in Fig. 1 (note that in this and subsequent figures, full lines represent interpolated curves, except when indicated). In a counterpart example,

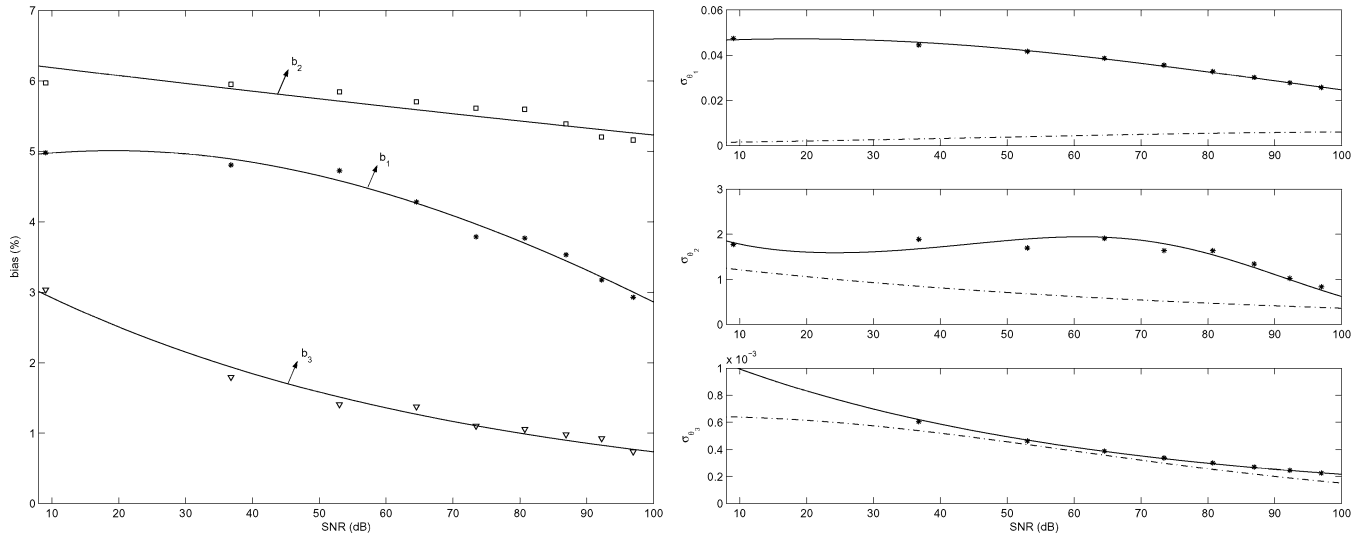


Fig. 3. Left: Bias of the MAP conductivity estimates as a function of SNR. Right: Standard deviations of these estimates (full lines) compared with the Cramér-Rao bound square roots (dashdotted lines).

we fixed SNR to 53 dB and varied the number of independent experiments used to compute  $\hat{\theta}_m$  and  $\sigma_{\theta_j}$ . The corresponding results are shown in Fig. 2.

The results of the previous examples show that it is possible to obtain asymptotically consistent estimates, even for low SNR values, with variances that approach the CRB for a sufficiently large number of experiments.

2) *Map Estimates*: We consider the case of a random parameter  $\theta$  distributed as  $\theta \sim \mathcal{N}(\bar{\theta}, \Upsilon)$ . Using a procedure similar to that in Section IV-A.I, we are now interested in calculating the MAP estimates of the conductivities for different SNR values. We study the bias and standard deviations of the estimates for a mean parameter prior  $\bar{\theta} = [0.3135, 226.19, 0.0121]^T$  (i.e., 5% away from the true value), and a relatively small uncertainty simulated by the following choice of independent parameter variances

$$\Upsilon = \begin{bmatrix} (0.05)^2 & 0 & 0 \\ 0 & 50^2 & 0 \\ 0 & 0 & (0.005)^2 \end{bmatrix}.$$

These values were selected to give our parameters a reliable *a priori* distribution.

We calculated the corresponding MAP estimates according to (15) and computed the bias of the mean estimate over the 200 experiments, and the corresponding standard deviations. The results are shown in the curves of Fig. 3. If we compare these results to those in Fig. 1, we note that an important improvement in the estimates can be achieved with the knowledge of a reliable prior. For the Bayesian approach, we were able to obtain estimates with low bias even for low SNR values, reducing their standard deviations (in comparison to those of the ML technique) and keeping them close to the stochastic CRB square roots.

### B. Sensitivity Analysis

The objective of the following numerical examples is to investigate the robustness of the MLE for different realistic conditions, such as errors in the source position or variations in the skull thickness.

1) *Sensitivity to Source Position Error*: We are interested in the effect of a small deterministic error  $\delta$  in the source position on the MLE. Define  $\delta$  as the distance between the nominal source position  $\mathbf{p}$  and the misspecified position  $\tilde{\mathbf{p}}$ , i.e.,  $\delta = \|\mathbf{p} - \tilde{\mathbf{p}}\|$ . Then, our experiment consisted of computing the MLE using  $\tilde{\mathbf{p}}$  instead of  $\mathbf{p}$ , allowing  $\delta$  to take values between 0 and 5 mm, under the condition that  $\|\tilde{\mathbf{p}}\| < \rho_1$ . Furthermore, we randomly chose the error  $\delta$  in various directions by using different magnitudes, azimuth, or elevation angles for  $\tilde{\mathbf{p}}$ .

For each value of  $\delta$ , we computed the MLE for 200 experiments with independent noise realizations and an SNR value of 80 dB. We chose this relatively high SNR value as we wanted to study the error introduced in the model due to  $\delta$  independently of the noise contribution. Then, we studied the effect of  $\delta$  on the bias and standard deviation of our estimates taking as reference the value at  $\delta = 0$  (no error), which corresponds to the case of an SNR = 80 dB in Fig. 1 and can be used in the current analysis as the least biased value and the one closest to the CRB.

Preliminary results showed that the second component of the conductivity estimate,  $\hat{\theta}_2$ , is dramatically affected by small errors in the source position, whereas the bias of other two estimates increases only moderately. However, high increments in  $b_2$  are produced not only by the position error, but also by an ill-posed condition during the estimation process. We tried to counteract this effect by replacing  $\theta_2$  with  $(\epsilon + 1/\theta_2)^{-1}$ , for a small value of  $\epsilon$ , in order to make the minimization process more robust to large changes in  $\theta_2$ . As result, both the bias and the standard deviations of our parameters were reduced significantly. These results are shown in Fig. 4 for  $\epsilon = 0.01$ .

2) *Sensitivity to Variations in the Skull Thickness*: Here, we wish to study the effect of variations in the skull thickness on the MLE of the conductivities. The skull thickness,  $\tau_2$ , is defined by the difference between the radii of the skull and CSF,  $\tau_2 = \rho_3 - \rho_2$ . An error in  $\tau_2$  is introduced by multiplying its nominal value by a factor  $\Delta\tau$ , leaving the thicknesses of the other two layers,  $\tau_1 = \rho_2 - \rho_1$  and  $\tau_3 = \rho_4 - \rho_3$ , unchanged. Therefore,  $\Delta\tau$  is defined as the proportion in which the true value of skull thickness is increased or decreased. For our experiments, we introduce different errors by multiplying  $\tau_2$  with values of  $\Delta\tau$

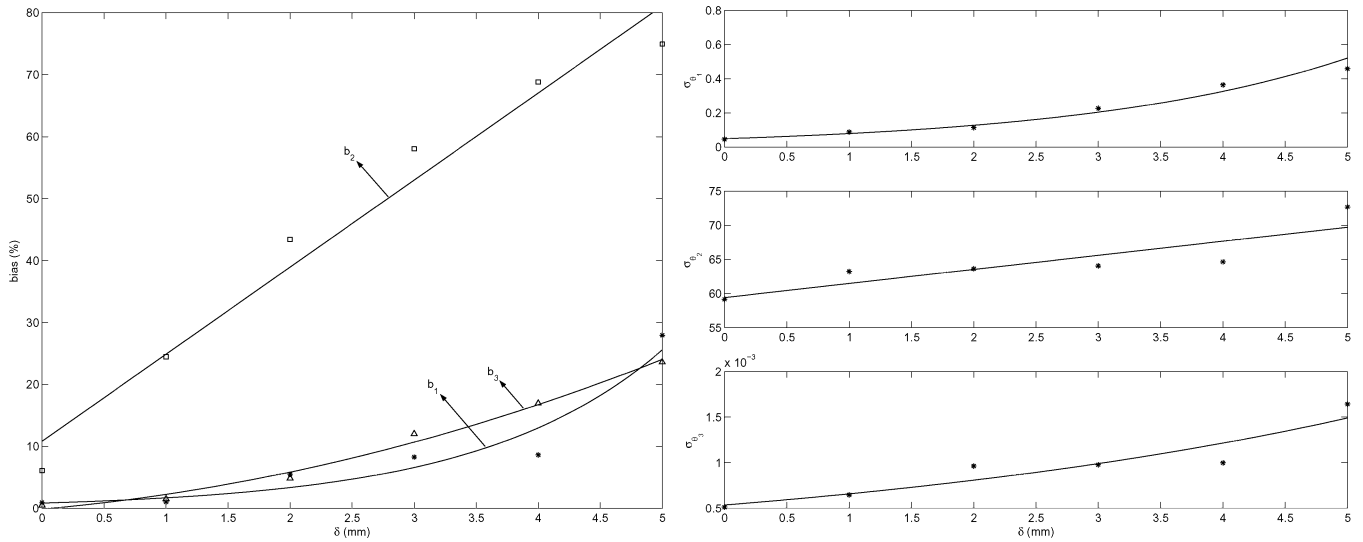


Fig. 4. Bias (left) and standard deviations (right) of the conductivity estimates as a function of source position error  $\delta$ . The value of the SNR is 80 dB and the number of experiments is 200.

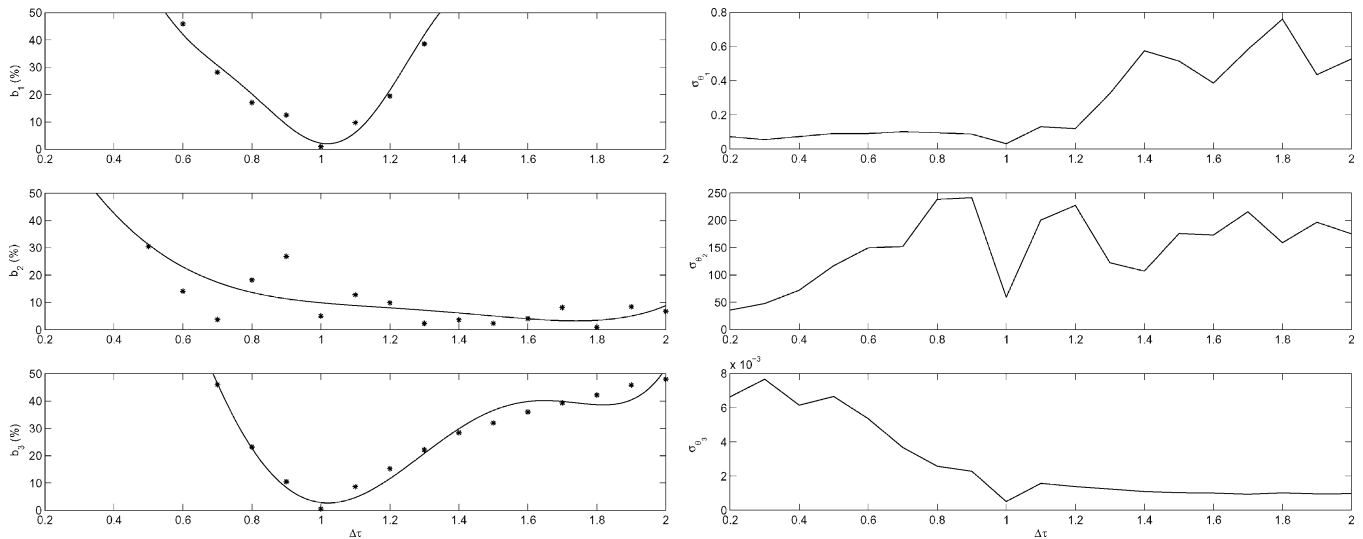


Fig. 5. Bias (left) and standard deviations (right, non interpolated) of the conductivity estimates as a function of  $\Delta\tau$ .

in the range of 0.2 to 2 (i.e., using one fifth to twice the true value of  $\tau_2$ ).

For each value of  $\Delta\tau$  we computed the MLE for 200 experiments with independent noise realizations and an SNR value of 80 dB. Next, we studied the effect of  $\Delta\tau$  on the bias and standard deviation of our estimates using as reference the value at  $\Delta\tau = 1$ , which corresponds to the nominal case and the point with smallest bias and closer to the CRB. The results shown in Fig. 5 indicate that our estimates can be sensitive to small changes in the skull thickness.

The way in which the estimates are affected differs in each case: Increments in the thickness of the skull ( $\Delta\tau > 1$ ) seem to reduce the bias in the estimate of  $\theta_2$  while keeping the same standard deviation. However, increasing the thickness of the skull obviously weakens the signals coming from the brain, making it more difficult to estimate  $\theta_1$  and  $\theta_3$ . By decreasing the thickness of the skull ( $\Delta\tau < 1$ ), we introduce errors in the head model, due to the change in the value of the different layers, increasing the bias of all estimates, even for small values of  $\Delta\tau$ .

### C. Real Data

In the following experiments, we compute the MLE of the conductivities and dipole source signals using real EEG and MEG data from two normal subjects. The data was recorded at the MEG center of Amsterdam, The Netherlands, using the Omega MEG/EEG system (CTF Systems Inc.), with 151 MEG channels and 64 EEG channels acquiring simultaneously the response to electrical stimulation of the median nerve. The frequency of the stimulus was set at 2 Hz and its duration at 0.2 ms. The intensity of the stimulation depended on the subject's sensitivity.

The stimulation was repeated to obtain 700 independent trials from each subject. The data was recorded at a rate of 1250 Hz with the electrodes positioned according to the extended 10–20 system. After acquisition, the data was band-pass filtered in the range [5,300] Hz. For the head, we used the 4-layer spherical model as in the previous experiments, but now the outer radius  $\rho_4$  was chosen to fit the scalp of each subject as close as possible.

Then, the radii of all layers were computed as  $[\rho_1, \rho_2, \rho_3, \rho_4] = [0.84, 0.8667, 0.9467, 1] \cdot \rho_4$ .

Next, we present two alternative procedures to obtain the estimates. In the first one, the source location is estimated using the MEG data and then the ML method is applied on the EEG data to compute the conductivities and source signals. In the second procedure, we present an iterative approach where only EEG data is used to compute the source location, the conductivities, and the source signals.

1) *MEG/EEG Data*: In these experiments, we used the MEG data to compute the estimate of the source position and then, using this estimate, calculate the MLE of the conductivities and dipole source signal from the EEG data.

For the estimation of the source, we used the ensemble average of the MEG data over the 700 trials and calculated the maximum variance (MV) estimate using the following expression [26]

$$\hat{\mathbf{p}} = \max_{\mathbf{p}} \text{tr} \left\{ \left[ H^T(\mathbf{p}) \hat{C}^{-1} H(\mathbf{p}) \right]^{-1} \right\} \quad (20)$$

where  $H(\mathbf{p})$  and  $\hat{C}$  are the array response matrix and sample covariance matrix, respectively, for the MEG case. A full description on how to compute  $H(\mathbf{p})$  can be found in [27]. An advantage of using MEG data is that  $H(\mathbf{p})$  is independent of the conductivities.

Equation (20) is equivalent to maximizing the variance or strength as a function of location within the volume of the brain, as regions of large variance presumably have substantial neural activity. In our case, the MV technique allows us to compute a source position estimate, independently of the ML technique, from averaged MEG data.

Once we have computed  $\hat{\mathbf{p}}$ , we use this estimate in our ML algorithm to compute  $\hat{\boldsymbol{\theta}}$  and  $\hat{\mathbf{q}}$  from the EEG data. Tables I and II summarize our results when using real data from a 25 years old female and a 40 years old male, respectively. In those tables, we show the values for  $\hat{\boldsymbol{\theta}}$ , the corresponding standard deviations compared to the CRB square roots, and  $\hat{\mathbf{p}}$ . Since  $\sigma^2$  in this case is not known, we computed the CRB using (9) by substituting  $\sigma^2$  with the estimate defined in (12) and  $Q(t)$  with  $\hat{Q}(t) = I_3 \otimes \hat{\mathbf{q}}(t)$ . The estimates of the dipole source signals are shown in Fig. 6.

Our results agree with those conductivity values reported in earlier studies using other methods [28], and support the belief that the ratio  $\theta_3$  is greater than the nominal value of 1/80 usually considered for the solution of the inverse problem. Furthermore, we note that the standard deviations of the conductivity estimates were close to the CRB square roots.

If we consider the results in [29], where the conductivity of the CSF was found to be  $\sigma_2 = 1.79$  S/m, we can compute the values of the remaining conductivities from our estimates. These results are shown in Table III.

2) *Iterative Procedure Using EEG Only*: Here we present an iterative procedure for the case when only EEG data is available. At each iteration, both the values of the source position and conductivities are updated. We assume that an approximate value of the source position is available (e.g., obtained from the topographic field map or from *a priori* information). In the first iteration, we use this approximate position and the nominal values of the conductivities to compute a better approximation for  $\mathbf{p}$ .

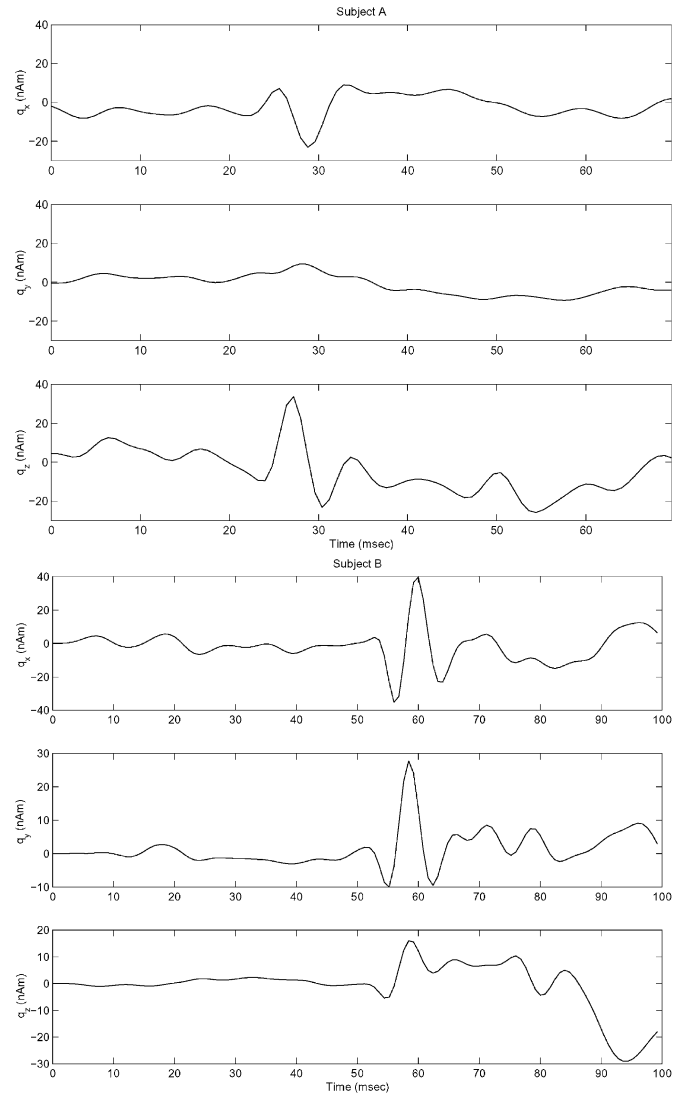


Fig. 6. Cartesian components of the estimated dipole source signals  $\hat{\mathbf{q}}(t)$  for each subject. These estimates were computed using (8) and the values of  $\hat{\boldsymbol{\theta}}$  described in Tables I and II for the MEG/EEG procedure.

This new approximation is obtained from (20) but with  $H(\mathbf{p})$  and  $\hat{C}$  replaced by  $A(\mathbf{p}, \boldsymbol{\theta})$  and  $\hat{R}$ , respectively. Note that for the estimation of the source position, we use the ensemble average of the EEG data over all the trials.

Once we have a better approximation of the source position, we proceed to estimate the conductivities with the ML technique using not all but a fraction of the total number of trials. In our case, we decided to use 100 different trials at each iteration to allow 7 iterations. With the resulting value of  $\boldsymbol{\theta}$ , we recalculate  $\mathbf{p}$  with the procedure explained before. We keep updating  $\boldsymbol{\theta}$  and  $\mathbf{p}$  until convergence is achieved.

We applied this procedure to the EEG data of both subjects. The results at the last iteration are shown also in Tables I and II, and the corresponding conductivity values for  $\sigma_2 = 1.79$  S/m are shown in Table III. We note that the algorithm achieved stable values for both the source position and conductivities at the fourth iteration, and the final values of these estimates are close to those obtained with the procedure described in Section IV-C.I, even when the initial position was about 3 cm away

TABLE I

RESULTS OBTAINED USING REAL DATA FROM A 25 YEARS OLD FEMALE SUBJECT. THIS TABLE SHOWS THE ESTIMATED RATIOS OF THE CONDUCTIVITIES, THEIR INDIVIDUAL STANDARD DEVIATIONS (SDs) AND CRB SQUARE ROOT IN PARENTHESIS, AND THE SOURCE LOCATION ESTIMATE, FOR BOTH THE MEG/EEG PROCEDURE AND THE ITERATIVE APPROACH USING ONLY EEG.

	$\hat{\theta}$	[0.1641, 159.5795, 0.0208] <sup>T</sup>		
MEG/EEG	(SD   $\sqrt{\text{CRB}}$ )	(0.0447   0.0391)	(38.32   18.89)	(0.0068   0.0051)
	$\hat{p}$	[0.224, -4.182, 8.673] <sup>T</sup> cm		
	$\hat{\theta}$	[0.1702, 159.6420, 0.0166] <sup>T</sup>		
EEG Only	(SD   $\sqrt{\text{CRB}}$ )	(0.0145   0.0042)	(27.78   20.38)	(0.0099   0.0045)
	$\hat{p}$	[0.187, -3.456, 8.164] <sup>T</sup> cm		

TABLE II

RESULTS OBTAINED USING REAL DATA FROM A 40 YEARS OLD MALE SUBJECT.

	$\hat{\theta}$	[0.1801, 139.0343, 0.0163] <sup>T</sup>		
MEG/EEG	(SD   $\sqrt{\text{CRB}}$ )	(0.007   0.0017)	(10.18   8.05)	(0.0025   0.0006)
	$\hat{p}$	[-0.441, -3.479, 8.963] <sup>T</sup> cm		
	$\hat{\theta}$	[0.1795, 139.266, 0.0156] <sup>T</sup>		
EEG Only	(SD   $\sqrt{\text{CRB}}$ )	(0.0068   0.0039)	(11.05   1.8232)	(0.0019   0.0005)
	$\hat{p}$	[-0.5906, -3.127, 8.996] <sup>T</sup> cm		

TABLE III

ESTIMATED VALUES OF THE CONDUCTIVITIES FOR  $\sigma_2 = 1.79$  S/m.

	Subject A	Subject B	
	$\hat{\sigma}_1$	0.2937 S/m	0.3223 S/m
MEG/EEG	$\hat{\sigma}_3$	0.0112 S/m	0.0128 S/m
	$\hat{\sigma}_4$	0.5393 S/m	0.7898 S/m
	$\hat{\sigma}_1$	0.3046 S/m	0.3213 S/m
EEG Only	$\hat{\sigma}_3$	0.0112 S/m	0.0128 S/m
	$\hat{\sigma}_4$	0.6755 S/m	0.8239 S/m

the final estimated position. This shows that the algorithm converges even for relatively large source position error.

## V. CONCLUSION

We have applied the ML method and Bayesian approach to estimate the conductivities of the different layers in the brain using EEG array measurements. We assumed a spherical head model and known dipole position. The last assumption may hold in practice for evoked response and event-related experiments.

Our simulations show that it is possible to obtain asymptotically consistent estimates, even for low SNR values, with variances that approach the CRB for a sufficiently large number of independent experiments. This assumption is valid as multiple experiments are feasible in practice. However, our method requires knowledge of the source position and geometry of the head, in order to avoid bias in the estimation process. One alternative to improve the estimation process is the Bayesian approach which allows using prior information on the distribution of the conductivity parameters.

Furthermore, we have shown how to extend our methods to the case of unknown positions by applying first MEG techniques, or by an iterative algorithm using EEG only. In the first

case, MEG is used independently to obtain an estimate of the source location. With this estimate, we proceeded to apply the ML technique using EEG data. However, when MEG data is not available, we proposed a second procedure where the source position and the conductivities were estimated and updated at multiple iterations using EEG only. Experiments with real MEG/EEG data were presented to show the applicability of both procedures. The results seem to be consistent with those reported in earlier studies.

Therefore, our methods have the potential of improving the accuracy of dipole estimates in practical cases, since the conductivities are usually unknown and vary among individuals. In addition, these methods have an easy implementation and allow a simultaneous estimation of the dipole signal, reducing the time required between experiments. Further research in this area will include more extensive application to real EEG data and realistic head modeling using numerical solutions such as BEM or FEM, as well as an analytical evaluation of the sensitivity.

## ACKNOWLEDGMENT

The authors thank Dr. J. C. de Munck and Dr. S. Gonçalves from the MEG center of Amsterdam, The Netherlands, for providing the real data used in this paper and for their helpful comments.

## REFERENCES

- [1] E. Niedermeyer and F. L. da Silva, "Electroencephalography," in *Basic Principles, Clinical Applications and Related Fields*. Baltimore, MD: Urban and Schwarzenberg Inc., 1987.
- [2] K. A. Awada, D. R. Jackson, S. B. Baumann, J. T. Williams, D. R. Wilton, P. W. Fink, and B. R. Prasky, "Effect of conductivity uncertainties and modeling errors on EEG source localization using a 2-D model," *IEEE Trans. Biomed. Eng.*, vol. 45, pp. 1135–1145, Sept. 1998.
- [3] T. F. Oostendorp, J. Delbeke, and D. F. Stegeman, "The conductivity of the human skull: Results of *in vivo* and *in vitro* measurements," *IEEE Trans. Biomed. Eng.*, vol. 47, pp. 1487–1492, Nov. 2000.

- [4] S. Gonçalves, J. C. de Munck, J. P. A. Verbunt, F. Bijma, R. Heethaar, and F. L. da Silva, "In vivo measurement of brain and skull resistivities using an EIT based method and realistic models for the head," *IEEE Trans. Biomed. Eng.*, vol. 50, pp. 754–767, June 2003.
- [5] S. Gonçalves, J. C. de Munck, J. P. A. Verbunt, R. Heethaar, and F. L. da Silva, "In vivo measurement of brain and skull resistivities using an EIT based method and the combined analysis of SEP/SEF data," *IEEE Trans. Biomed. Eng.*, vol. 50, pp. 1124–1127, Sept. 2003.
- [6] E. Jonsson, "Electrical conductivity reconstruction using nonlocal boundary conditions," *SIAM Journal on Applied Mathematics*, vol. 59, no. 5, pp. 1582–1598, 1999.
- [7] D. S. Tuch, V. J. Wedeen, A. M. Dale, J. S. George, and J. W. Belliveau, "Conductivity tensor mapping of the human brain using diffusion tensor MRI," *Proceedings of the National Academy of Sciences of the United States of America*, vol. 98, no. 20, pp. 11 697–11 701, 2001.
- [8] H. M. Huizenga, T. L. Van Zijden, D. J. Heslenfeld, and P. C. M. Molenaar, "Simultaneous MEG and EEG source analysis," *Physics in Medicine and Biology*, vol. 46, no. 1, pp. 1737–1751, 2001.
- [9] D. Gutiérrez, A. Nehorai, C. Muravchik, and J. Lewine, "Estimating conductivities and dipole source signal with EEG arrays," in *Proceedings of the 13th International Conference on Biomagnetism*, Jena, Germany, 2002, pp. 700–702.
- [10] B. N. Cuffin and D. Cohen, "Comparison of the magnetoencephalogram and electroencephalogram," *Electroencephalography and Clinical Neurophysiology*, vol. 47, no. 1, pp. 132–146, 1979.
- [11] C. A. Brebbia and J. Dominguez, *Boundary Elements. An Introduction Course*. New York: McGraw-Hill, 1992.
- [12] K. H. Huebner, E. A. Thornton, and T. G. Byrom, *The Finite Element Method for Engineers*. New York: John Wiley & Sons, 1995.
- [13] J. W. Rohrbaugh, R. Parasuraman, and R. Johnson, *Event - Related Brain Potentials: Basic Issues and Applications*. New York: Oxford Univ. Press, 1990.
- [14] B. Hochwald and A. Nehorai, "Magnetoencephalography processing with diversely-oriented and multi-component sensors," *IEEE Trans. Biomed. Eng.*, vol. 44, pp. 40–50, Jan. 1997.
- [15] A. Dogandzic and A. Nehorai, "Estimating evoked dipole responses in unknown spatially correlated noise with EEG/MEG arrays," *IEEE Trans. Signal Processing*, vol. 48, pp. 13–25, Jan. 2000.
- [16] M. G. Kendall and A. Stuart, *The Advanced Theory of Statistics*. New York: Hafner, 1961.
- [17] H. L. Van Trees, *Detection, Estimation, and Modulation Theory, Part I*. New York: Wiley, 1968.
- [18] C. Muravchik and A. Nehorai, "EEG/MEG error bounds for a static dipole source with a realistic head model," *IEEE Trans. Signal Processing*, vol. 49, pp. 470–484, Mar. 2001.
- [19] D. A. Brody, F. H. Terry, and R. E. Ideker, "Eccentric dipole in a spherical medium: Generalized expression for surface potentials," *IEEE Trans. Biomed. Eng.*, vol. BME-20, pp. 141–143, 1973.
- [20] Y. Salu, L. G. Cohen, D. Rose, S. Sato, C. Kufta, and M. Hallett, "An improved method for localizing electric brain dipoles," *IEEE Trans. Biomed. Eng.*, vol. 37, pp. 699–705, July 1990.
- [21] P. Stoica and T. Soderstrom, "Parameter identifiability," *IEE Proc. Radar, Sonar and Navig.*, vol. 141, no. 3, pp. 133–136, 1994.
- [22] P. Stoica and A. Nehorai, "MUSIC, maximum likelihood, and Cramer-Rao bound," *IEEE Trans. Acoust., Speech, Signal Processing*, vol. 37, pp. 720–741, May 1989.
- [23] B. M. Radich and K. M. Buckley, "EEG dipole localization bounds and map algorithms for head models with parameter uncertainties," *IEEE Trans. Biomed. Eng.*, vol. 42, pp. 233–241, Mar. 1995.
- [24] M. Sun, "An efficient algorithm for computing multishell spherical volume conductor models in EEG dipole source localization," *IEEE Trans. Biomed. Eng.*, vol. 44, pp. 1243–1252, Dec. 1997.
- [25] V. L. Towle and J. Bolanos, "The spatial location of EEG electrodes: Locating the best-fitting sphere relative to cortical anatomy," *Electroencephalogr. Clin. Neurophysiol.*, vol. 86, no. 1, pp. 1–6, 1993.
- [26] B. D. Van Veen, W. Van Drongelen, M. Yuchtman, and A. Suzuki, "Localization of brain electrical activity via linearly constrained minimum variance spatial filtering," *IEEE Trans. Biomed. Eng.*, vol. 44, pp. 867–880, Sept. 1997.
- [27] M. Hämmäläinen, R. Hari, R. J. Ilmoniemi, J. Knuutila, and O. V. Lounasmaa, "Magnetoencephalography – Theory, instrumentation, and applications to noninvasive studies of the working human brain," *Rev. Moder Phys.*, vol. 65, no. 2, pp. 413–497, 1993.
- [28] T. C. Ferre, K. J. Eriksen, and D. M. Tucker, "Regional head tissue conductivity estimation for improved EEG analysis," *IEEE Trans. Biomed. Eng.*, vol. 47, pp. 1584–1592, Dec. 2000.
- [29] S. B. Baumann, D. R. Wozny, S. K. Kelly, and F. Meno, "The electrical conductivity of human cerebrospinal fluid at body temperature," *IEEE Trans. Biomed. Eng.*, vol. 44, pp. 220–223, Mar. 1997.



**David Gutiérrez** received the B.Sc. degree (with honors) in electrical engineering from the National Autonomous University of Mexico (UNAM), Mexico, in 1997 and the M.Sc. degree in electrical engineering and computer sciences from the University of Illinois, Chicago (UIC), in 2000. He is currently working towards the Ph.D. degree in the Bioengineering Department at UIC.

His research interests are in statistical signal processing and its applications to biomedicine. He is also interested in image processing, neurosciences, real-

time algorithms, and ultrasound. Mr. Gutiérrez held the Fulbright Fellowship of the Foreign Graduate Program 1998–2001, and he has been a fellow of the National Council for Science and Technology (CONACYT), Mexico, during all his graduate studies at UIC.



**Arye Nehorai** (S'80–M'83–SM'90–F'94) received the B.Sc. and M.Sc. degrees in electrical engineering from the Technion, Israel, and the Ph.D. degree in electrical engineering from Stanford University, Stanford, CA.

After graduation he worked as a Research Engineer for Systems Control Technology, Inc., in Palo Alto, CA. From 1985 to 1989 he was Assistant Professor and from 1989 to 1995 he was Associate Professor with the Department of Electrical Engineering at Yale University. In 1995 he joined the Department

of Electrical Engineering and Computer Science at The University of Illinois at Chicago (UIC), as a Full Professor. From 2000 to 2001 he was Chair of the department's Electrical and Computer Engineering (ECE) Division, which is now a new department. In 2001 he was named University Scholar of the University of Illinois. He holds a joint professorship with the ECE and Bioengineering Departments at UIC. His research interests are in signal processing, communications, and biomedicine.

Dr. Nehorai Vice President-Publications and Chair of the Publications Board of the IEEE Signal Processing Society. He is also a member of the Board of Governors and of the Executive Committee of this Society. He was Editor-in-Chief of the IEEE TRANSACTIONS ON SIGNAL PROCESSING from January 2000 to December 2002, and is currently a Member of the Editorial Board of *Signal Processing*, the *IEEE Signal Processing Magazine*, and *The Journal of the Franklin Institute*. He is the founder and Guest Editor of the special columns on Leadership Reflections in the *IEEE Signal Processing Magazine*. He has previously been an Associate Editor of the IEEE TRANSACTIONS ON ACOUSTICS, SPEECH AND SIGNAL PROCESSING, the IEEE SIGNAL PROCESSING LETTERS, the IEEE TRANSACTIONS ON ANTENNAS AND PROPAGATION, the IEEE JOURNAL OF OCEANIC ENGINEERING, the IEEE JOURNAL OF OCEANIC ENGINEERING and *Circuits, Systems, and Signal Processing*. He served as Chairman of the Connecticut IEEE Signal Processing Chapter from 1986 to 1995, and a Founding Member, Vice-Chair and later Chair of the IEEE Signal Processing Society's Technical Committee on Sensor Array and Multichannel (SAM) Processing from 1998 to 2002. He was the co-General Chair of the First and Second *IEEE SAM Signal Processing Workshops* held in 2000 and 2002. He was co-recipient, with P. Stoica, of the 1989 IEEE Signal Processing Society's Senior Award for Best Paper, and co-author of the 2003 Young Author Best Paper Award of this Society, with A. Dogandzic. He received the Faculty Research Award from the UIC College of Engineering in 1999 and was Adviser of the UIC Outstanding Ph.D. Thesis Award in 2001. He was elected Distinguished Lecturer of the IEEE Signal Processing Society for the term 2004 to 2005. He has been a Fellow of the Royal Statistical Society since 1996.



**Carlos H. Muravchik** (S'81–M'83–SM'99) was born in Argentina, June 11, 1951. He graduated as an Electronics Engineer from the National University of La Plata, La Plata, Argentina, in 1973. He received the M.Sc. in statistics (1983) and the M.Sc. (1980) and Ph.D. (1983) degrees in electrical engineering, from Stanford University, Stanford, CA.

He is currently a Professor at the Department of the Electrical Engineering of the National University of La Plata and a member of its Industrial Electronics, Control and Instrumentation Laboratory (LEICI). He is also a member of the Comision de Investigaciones Cientificas de la Pcia. de Buenos Aires. He was a Visiting Professor at Yale University, New Haven, CT, in 1983 and 1994, and at the University of Illinois at Chicago in 1996, 1997, 1999, and 2003. His research interests are in the area of statistical signal and array processing with biomedical, control, and communications applications, and nonlinear control systems.